2009 American Control Conference
Hyatt Regency Riverfront, St. Louis, MO, USA
June 10-12, 2009

On the Computation of Compatible Trajectories for Hydraulic Shaketables

John Hauser and M. V. Sivaselvan

Abstract— **Dynamic testing is often used to study the response of structures under earthquake loading. Such testing is either carried out with a prescribed input such as an earthquake ground motion, or using computation-in-the-loop, where a physical substructure is made to interact with a virtual substructure. This latter form of dynamic testing is also referred to as hybrid simulation. In both cases, the test system consisting of the physical test-piece, the actuators and sensors, controls, and other computations, constitutes a dynamic system that is different from the structure whose behavior is the focus of the test. It is therefore of interest to ask if there are trajectories of the test system that are compatible with desired trajectories of the structure tested. In this paper, we formulate this problem of finding compatible trajectories, as a nonlinear least-squares problem, and propose optimization strategies. We discuss the trajectory computation with two examples, seismic testing with prescribed ground motion, and hybrid simulation with a shaketable as the transfer system.**

I. INTRODUCTION

Laboratory dynamic testing is widely employed to study the behavior of structures under earthquake loading. A review of different dynamic testing methodologies can be found in [1]. A commonly used technique is shaketable testing, where a model of a structure is mounted on a platform, and the platform is shaken so as to replicate a suitable prescribed earthquake ground motion. The platform is most often driven by servo-hydraulic actuators, and control strategies are used to try to make the platform track the desired ground motion.

Dynamic testing is also performed with computation-in-the-loop. Here, models are created that consist of two parts actively interacting during the test: (a) a physical subsystem - an experimental component representing a portion of a system and (b) a virtual subsystem - a computer model of the remainder of the system. The interface conditions between the two substructures are imposed by a transfer system, often a servo-hydraulic actuator. This technique of combining physical and virtual components has been termed hybrid simulation.

In this paper, we consider shaketable seismic testing, and a form of hybrid simulation where the transfer system is a shaketable. In either case, the test system consisting of the physical test-piece, the shaketable with its mechanical and hydraulic components, controls, and perhaps computation-in-the-loop, constitutes a dynamic system that is substantially different from the structure whose behavior is the focus of the test. It is therefore of interest to know what trajectories of the test system comprise behavior of the test structure that we seek to observe. We call trajectories of the test system that comprise the desired behavior of the test structure, compatible trajectories. It is not necessary that there exists a compatible trajectory of the test system for any desired trajectory of the test structure. Here, we propose a strategy based on optimization to seek out compatible trajectories of the test system. If such compatible trajectories exist, then the design of online controls for dynamic tests can be meaningfully explored.

This work was supported by MTS Systems Corp.

John Hauser is with Department of Electrical and Computer Engineering, University of Colorado at Boulder, Boulder, CO 80309, USA hauser@colorado.edu

M. V. Sivaselvan is with the Department of Civil, Environmental and Architectural Engineering, University of Colorado at Boulder, Boulder, CO 80309, USA siva@colorado.edu

II. COMPATIBLE TRAJECTORIES FOR TESTING WITH PRESCRIBED INPUT

We consider a system as being modeled by a nonlinear differential equation,

$$\dot{x} = f(x, w) \tag{1}$$

where x is the vector of states of the system, and w is the vector of external disturbances, such as earthquake ground motion. For dynamic testing, we couple this system with a device such as a shaketable. The mathematical model of the coupled system is of the form

$$\begin{aligned} \dot{x} &= \bar{f}\,(x, x_a, u) \\ \dot{x}_a &= f_a\,(x, x_a, u) \end{aligned} \tag{2}$$

where x_a is the state of the actuators and u is a control input. The differential equation for x is modified due to the interaction of the test structure with the actuators. Let $g(x_a, u)$ be an output function that plays the role of the disturbance w in the original model. We pose the problem of determining compatible trajectories of the test system as a nonlinear least-squares optimization problem,

$$\begin{aligned} &\min \frac{1}{2}\left(||x(\cdot) - x_d(\cdot)||^2 + ||g(x_a(\cdot), u(\cdot)) - w_d(\cdot)||^2 + ||u(\cdot)||^2\right) \\ &\text{subject to the system dynamics of equation (2)} \end{aligned} \tag{3}$$

where $w_d(\cdot)$ is the desired external disturbance, and x_d is a desired trajectory of the system that might have been obtained from a numerical simulation.

III. COMPATIBLE TRAJECTORIES FOR HYBRID SIMULATION

Hybrid simulation is the technique of combining physical and virtual components to study the dynamic behavior of complex engineering structures. We again consider a system

978-1-4244-4524-0/09/$25.00 ©2009 AACC

as being modeled by (1). In order to examine its behavior, we dissect the system, i.e., we partition its states as

$$\begin{aligned} \dot{x}_1 &= f_1(x_1, x_2, w) \\ \dot{x}_2 &= f_2(x_1, x_2, w) \end{aligned} \tag{4}$$

We choose to build a physical representation of one of these subsystems, say x_1, which we consider more critical, or which wish to understand more about, and keep the other subsystem virtual. To stick them back together, we need some *glue*, to get the state x_1 into the x_2 subsystem, and the state x_2 into the x_1 subsystem. This glue is provided by sensors, actuators, controls, and by an understanding of the system objectives and of the global nonlinear dynamics. Here for simplicity, we assume direct physical measurement of all physical states. The mathematical model of the system after it is glued back together is

$$\begin{aligned} \dot{x}_1 &= \bar{f}_1(x_1, x_a, w, u) \\ \dot{x}_2 &= f_2(x_1, x_2, w) \\ \dot{x}_a &= f_a(x_1, x_a, u) \end{aligned} \tag{5}$$

which now includes the dynamics of the sensors and the actuators. x_a is the state of the actuators and sensors and u is a control input to the system. The differential equation for x_1 is also modified due to the interaction of the physical subsystem with the actuators. We wish to determine trajectories of the hybrid system (5) that are compatible with trajectories of the full emulated system (4). We again pose this as a nonlinear least-squares optimization problem as follows.

$$\begin{aligned} &\min \frac{1}{2}\left(||x(\cdot) - x_d(\cdot)||^2 + ||w(\cdot) - w_d(\cdot)||^2 + ||u(\cdot)||^2\right) \\ &\text{subject to the system dynamics of equation (5)} \end{aligned} \tag{6}$$

where $w_d(\cdot)$ and x_d are as defined before.

IV. HYDRAULIC SHAKETABLE MODEL

We present a nonlinear mathematical model of a uniaxial shaketable, which we will use in the examples that follow. We follow the modeling practices of [2] and [3], but pay special attention to features that are important for the trajectory optimization strategies. A schematic of a shaketable driven by a hydraulic actuator fitted with a servovalve is shown in Figure 1. Denoting by x and v the position and velocity of the table, assuming that the actuator is attached rigidly to an inertial frame, and ignoring all frictional resistance to the motion of the table, we see immediately that

$$\dot{x} = v; \qquad \dot{v} = \frac{A_p}{M_t}(P_1 - P_2) \tag{7}$$

where P_1 and P_2 are the pressures in the two actuator chambers as shown in the figure, and A_p and M_t are respectively the area of the piston and the mass of the table. Conservation of mass of oil in each of the two actuator chambers gives

$$\begin{aligned} Q_1 - Q_2 &= \frac{A_p(x_0 + x)}{\kappa}\dot{P}_1 + K_l(P_1 - P_2) + A_p v \\ Q_4 - Q_3 &= \frac{A_p(x_0 - x)}{\kappa}\dot{P}_2 - K_l(P_1 - P_2) - A_p v \end{aligned} \tag{8}$$

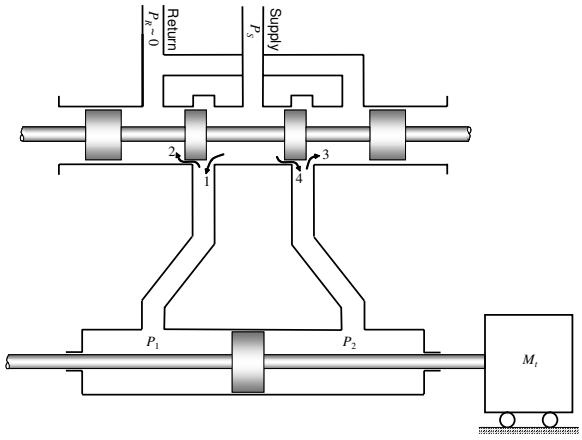

Fig. 1. Schematic of a hydraulic shaketable

where Q_i is the flow through port i of the servovalve, x_0 is half the stroke of the actuator, and K_l is a leakage coefficient (we model the leakage flow between the two chambers around the piston to be proportional to the pressure difference between the chambers). The flows Q_i depend on the valve spool position, and on the pressure difference across the the respective port. For simplicity, we ignore here the valve dynamics, and consider the valve spool position to be the control input.

Considering $\chi_1 = x$, $\chi_2 = v$, $\chi_3 = P_1$ and $\chi_4 = P_2$ as states, equations (7) and (8) result in the following system of differential equations.

$$\begin{aligned} \dot{\chi}_1 &= \chi_2 \\ \dot{\chi}_2 &= \frac{A_p}{M_t}(\chi_3 - \chi_4) \\ \dot{\chi}_3 &= \frac{\kappa}{A_p(x_0 + \chi_1)}(Q(P_S - \chi_3, u) - Q(\chi_3 - P_R, -u) \\ &\qquad - K_l(\chi_3 - \chi_4) - A_p\chi_2) \\ \dot{\chi}_4 &= \frac{\kappa}{A_p(x_0 - \chi_1)}(Q(P_S - \chi_4, -u) - Q(\chi_4 - P_R, u) \\ &\qquad + K_l(\chi_4 - \chi_3) + A_p\chi_2) \end{aligned} \tag{9}$$

where, u, the valve spool position is the control input, and P_S and P_R are the supply and return pressures.

A. Orifice Flow Function

Commonly, an equation obtained from Bernoulli's principle, and applicable to high Reynolds number flows, is used to describe the flow through the servovalve ports over the entire range of pressure differences and valve openings. While this is a reasonable approximation since orifice flow is predominantly turbulent, it causes two mathematical difficulties:

1) The resulting differential equations do not satisfy a Lipschitz condition when the pressure drop across the orifice is zero.
2) The pressure-flow equation is non-smooth when valve spool displacement is zero.

These difficulties however do not arise if we account for the following facts:

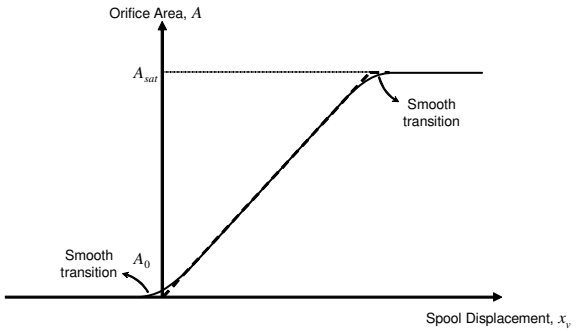

Fig. 2. Orifice area – spool displacement relationship

1) The orifice flow is *laminar* when the pressure drop or valve opening is small (i.e. low Reynolds numbers).
2) In *real* valves, there is clearance between the spool and the landings, so that there is some *leakage* flow even when the valve displacement is zero.

With these considerations, we represent the orifice area as a function of the valve spool displacement with smooth transitions as shown in Figure 2. The smooth transitions may be obtained using interpolation with Hermite polynomials, matching as many derivatives as desired with the straight line segments at either end of the interval. The orifice pressure-flow equation is given by

$$\begin{aligned} &Q(P, x_v) \\ &= \left(\sqrt{k_1(x_v)P\tanh\alpha P + k_2(x_v)^2} - k_2(x_v)\right)\tanh\alpha P \\ &+ \frac{1}{2}\frac{k_1(x_v)}{k_2(x_v)}\left(1-\tanh^2\alpha P\right) \end{aligned} \tag{10}$$

where P is the pressure drop across the orifice, x_v is the spool displacement, $k_1(x_v) = C_d^2 A(x_v)^2\frac{2}{\rho}$, $k_2(x_v) = \frac{\nu R_{tr}}{2b(x_v)}$, $A(x_v)$ is the area of the orifice, $b(x_v) = \frac{2w}{w^2+A(x_v)}$, w is the orifice width, C_d is the turbulent flow discharge coefficient of the orifice, R_{tr} is the Reynolds number at which the flow transitions from laminar to turbulent, ρ is the density of the hydraulic oil, ν is the coefficient of viscosity of the hydraulic oil. α is a parameter such that the larger its value, the smaller the norm $||\text{sgn}(x) - \tanh\alpha x||_1$. Equation (10) has been obtained by modifying an empirical flow equation proposed in [4], in such a way that $Q(\cdot,\cdot)$ is as differentiable as the smooth transitions in Figure 2.

B. Equilibrium Points and Linearization

The equilibrium points of the differential equation (9) for $u = 0$ are $\chi_1 \in (-x_0, x_0)$, $\chi_2 = 0$, $\chi_3 = \chi_4 = \frac{P_S+P_R}{2}$. Linearization about the midstroke equilibrium point (i.e., $\chi_1 = 0$) gives

$$\dot{\zeta} = A\zeta + B\nu \tag{11}$$

where

$$A = \begin{bmatrix} 0 & 1 & 0 & 0 \\ 0 & 0 & a & -a \\ 0 & -b & -(c+d) & d \\ 0 & b & d & -(c+d) \end{bmatrix}$$

and $B = \begin{bmatrix} 0 & 0 & e & -e \end{bmatrix}^T$ with $a = \frac{A_p}{M_t}$, $b = \frac{\kappa}{x_0}$, $d = \frac{\kappa}{A_p x_0}K_l$ and $c, e = \frac{\kappa}{A_p x_0}\left[2D_{1,2}Q\left(\frac{P_S+P_R}{2}, 0\right)\right]$. The operator D_i denotes the partial derivative with respect to argument i. The eigenvalues of this linearization are $\lambda_1 = 0$, $\lambda_{2,3} = \frac{1}{2}\left(-(c+2d) \pm i\sqrt{8ab-c^2}\right)$ and $\lambda_4 = -c$ with corresponding eigenvectors, $v_1 = \{1,0,0,0\}^T$, $v_{2,3} = \left\{-\frac{-\alpha_1 \pm i\alpha_2}{b(-\alpha_1 \mp i\alpha_2)}, -\frac{-\alpha_1 \pm i\alpha_2}{2b}, -1, 1\right\}^T$ and $v_4 = \{0,0,1,1\}^T$, where $\alpha_1 = c + 2d$ and $\alpha_2 = \sqrt{8ab-(c+2d)^2}$. The complex conjugate pair of eigenvalues correspond to the well-known *oil-column* resonance.

$$\omega = \sqrt{\frac{2\kappa A_p}{x_0 M_t}}; \quad \xi = \sqrt{\frac{\kappa M_t}{2A_p x_0}}\frac{\left[D_1 Q\left(\frac{P_S+P_R}{2}, 0\right) + K_l\right]}{A_p}$$

are the frequency and damping ratio of this resonance.

C. Coordinate Transformation

Let $\Phi = [v_1 v_2 v_3 v_4]$. It can be seen that the fourth row of $\Phi^{-1}B$ is zero. Therefore, the mode v_4 is stable and *uncontrollable*. This motivates a coordinate transformation so that the sum of the chamber pressures is a state. We choose the following linear coordinate transformation,

$$T = \begin{bmatrix} 1 & 0 & 0 & 0 \\ 0 & 1 & 0 & 0 \\ 0 & 0 & 1 & -1 \\ 0 & 0 & 1 & 1 \end{bmatrix}$$

The new coordinate, $x = T\chi$ are $x_1 = \chi_1$, the table displacement, $x_2 = \chi_2$, the table velocity, $x_3 = P_1 - P_2$, the differential pressure, and $x_4 = P_1 + P_2$, the sum of the chamber pressures. In these transformed coordinates, the dynamics of the shaking table can be described by the following system of nonlinear differential equations.

$$\begin{aligned} \dot{x}_1 &= x_2 \\ \dot{x}_2 &= \frac{A_p}{M_t}x_3 \\ \dot{x}_3 &= f_3(x_1, x_2, x_3, x_4, u) \\ \dot{x}_4 &= f_4(x_1, x_2, x_3, x_4, u) \end{aligned} \tag{12}$$

where

$$\begin{aligned} &f_3(x_1, x_2, x_3, x_4, u) \\ &= \frac{\kappa}{A_p(x_0^2 - x_1^2)}\left(x_0 Q_I(x_3, x_4, u) - x_1 Q_{II}(x_3, x_4, u)\right. \\ &\qquad \left. -2K_l x_0 x_3 - 2A_p x_0 x_2\right) \\ &f_4(x_1, x_2, x_3, x_4, u) \\ &= \frac{\kappa}{A_p(x_0^2 - x_1^2)}\left(x_0 Q_{II}(x_3, x_4, u) - x_1 Q_I(x_3, x_4, u)\right. \\ &\qquad \left. +2K_l x_1 x_3 + 2A_p x_1 x_2\right) \end{aligned}$$

where Q_I and Q_{II} are combinations of flows in the four ports of the servovalve, and are given by

$$Q_{I,II}(x_3, x_4, u) = Q(p_1, u) - Q(p_2, -u) \pm Q(p_3, u) \mp Q(p_4, -u)$$

where p_i is the pressure drop across orifice i. Thus $p_1 = P_S - \frac{x_3+x_4}{2}$, $p_2 = \frac{x_3+x_4}{2} - P_R$, $p_3 = \frac{x_4-x_3}{2} - P_R$ and $p_4 =$

$P_S - \frac{x_4 - x_3}{2}$. $Q(\cdot,\cdot)$ is the orifice flow function of equation (10). It is also interesting to note the following symmetry.

$$D_1 Q_I(x_3, x_4, u) = D_2 Q_{II}(x_3, x_4, u)$$
$$D_2 Q_I(x_3, x_4, u) = D_1 Q_{II}(x_3, x_4, u)$$

V. EXAMPLE I — UNIAXIAL SHAKETABLE TRAJECTORY COMPATIBLE WITH AN ACCELEROGRAM

In this example, we compute a trajectory of a uniaxial shaketable that is compatible with a prescribed ground motion accelerogram. We first obtain a desired trajectory by computing position and velocity curves that are consistent with given accelerogram. We then compute a compatible trajectory of the shaketable by optimization.

A. Constructing Compatible Position and Velocity Curves for an Accelerogram

A number of heuristics are commonly used to obtain position and velocity curves that are consistent with a given accelerogram. Here, we use an optimization-based heuristic. Given an accelerogram $a(\cdot)$, we obtain consistent position and velocity curves by solving the quadratic optimization problem,

$$\min_{(x(\cdot),u(\cdot))} \frac{1}{2}\int_0^T ||x(\tau)||_Q^2 + ||u(\tau)||_R^2 \, d\tau + \frac{1}{2}||x(T)||_{P_1}^2$$

Subject to

$$\dot{x} = Ax + B\left(a(t) + u\right); \quad x(0) = 0 \tag{13}$$

where x is the vector of position and velocity, $A = [0, 1; 0, 0]$ and $B = [0, 1]^T$. Q and R are suitably chosen weights. P_1 is obtained by solving the corresponding algebraic Riccati equation. The solution to (13) is this an LTI backward and forward filtering of $a(\cdot)$. One might also add position and velocity-acceleration constraints to (13) to take into account limits of the shaketable in constructing compatible position and velocity curves. Position and velocity curves consistent with the 1940 El Centro accelerogram computed using the optimization strategy proposed above are labeled "Desired" in Figures 3(a) and 3(b) respectively.

B. Trajectory Optimization and Selection of Weights

We now set out to compute a trajectory of the shaketable that is consistent with the desired position, velocity and acceleration curves computed above. The desired curve for the differential pressure state is set to M_t/A_p times the desired acceleration, and desired curve for the sum of the pressures state is set to be the zero curve. A compatible trajectory is computed by solving the following least-squares optimization problem.

$$\min_{(x(\cdot),u(\cdot))} \frac{1}{2}\int_0^T ||x(\tau) - x_d(\tau)||_Q^2 + ||u(\tau) - u_d(\tau)||_R^2 \, d\tau + \frac{1}{2}||x(T) - x_d(T)||_{P_1}^2$$

Subject to the dynamics of equation (12) (14)

The positive definite weights Q and R are chosen to obtain desirable transient dynamics. A controller is first designed based on pole placement of the linearized dynamics. An inverse optimal control problem is solved using convex optimization to obtain Q and R [5]. The optimization problem is solved using a projection operator-based descent algorithm [6]. Compatible trajectories of the shaketable computed for the 1940 El Centro accelerogram are shown in Figure 3

VI. EXAMPLE II — COMPATIBLE TRAJECTORY FOR HYBRID SIMULATION

In this example, we consider hybrid simulation with uniaxial shaking tables and look at periodic trajectories in particular. The full system to be emulated, is a two-story building constrained to move in one plane. An eccentric mass shaker mounted on the top floor, provides periodic excitation to the building. We hybridize the system as shown schematically in figure 4, keeping the top floor physical, and modeling the bottom floor virtually. We ask if this hybrid system, when excited by the eccentric mass shaker, can be made by means of suitable controls, to exhibit the same periodic trajectories as the full emulated system.

A. Full Physical System Model

We model the full emulated system shown in the upper part of Figure 4 by the following linear differential equations.

$$\begin{aligned}
\dot{x}_1 &= x_2 \\
\dot{x}_2 &= -\frac{c_1 + c_2}{m_1}x_2 + \frac{c_2}{m_1}x_6 - \frac{k_1 + k_2}{m_1}x_1 + \frac{k_2}{m_1}x_5 \\
\dot{x}_5 &= x_6 \\
\dot{x}_6 &= \frac{c_2}{m_2}x_2 - \frac{c_2}{m_2}x_6 + \frac{k_2}{m_2}x_1 - \frac{k_2}{m_2}x_5 + \frac{1}{m_2}w(t)
\end{aligned} \tag{15}$$

where the states x_1 and x_2 are the displacement and velocity of the first floor and x_5 and x_6 are those of the second floor, m_i, c_i and k_i are the mass, damping and stiffness of floor i and $w(t)$ is the force applied by the eccentric mass shaker.

B. Hybrid System Model

The model of the hybrid system shown in the bottom part of Figure 4 is

$$\begin{aligned}
\dot{x}_1 &= x_2 \\
\dot{x}_2 &= \frac{A_p}{M_t}x_3 - \frac{c_2}{M_t}x_2 + \frac{c_2}{m_1}x_6 - \frac{k_1 + k_2}{m_1}x_1 + \frac{k_2}{m_1}x_5 \\
\dot{x}_3 &= f_3\left(x_1, x_2, x_3, x_4, u\right) \\
\dot{x}_4 &= f_4\left(x_1, x_2, x_3, x_4, u\right) \\
\dot{x}_5 &= x_6 \\
\dot{x}_6 &= \frac{c_2}{m_2}x_2 - \frac{c_2}{m_2}x_6 + \frac{k_2}{m_2}x_1 - \frac{k_2}{m_2}x_5 + \frac{1}{m_2}w(t)
\end{aligned} \tag{16}$$

where the states, inputs and parameters are as described for the shaking table and for the full emulated system.

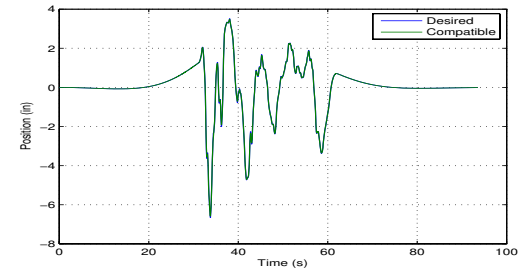

(a) Position

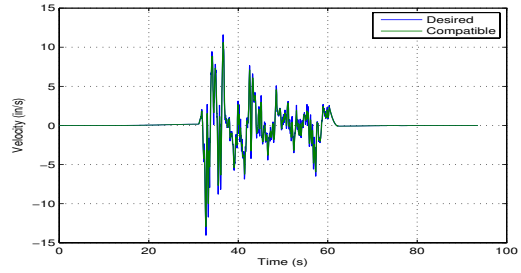

(b) Velocity

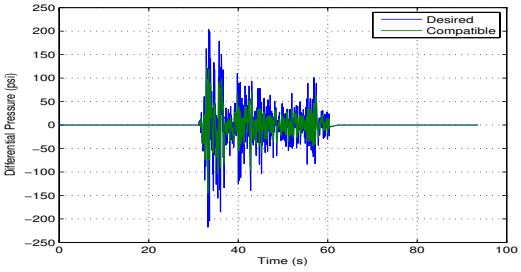

(c) Differential Pressure

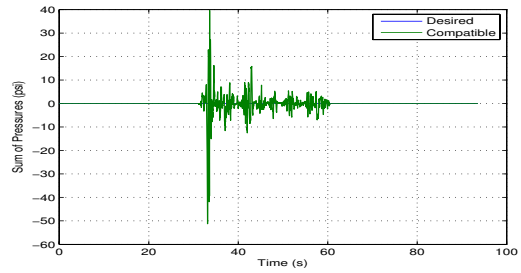

(d) Sum of Pressures (variation about 3000 psi)

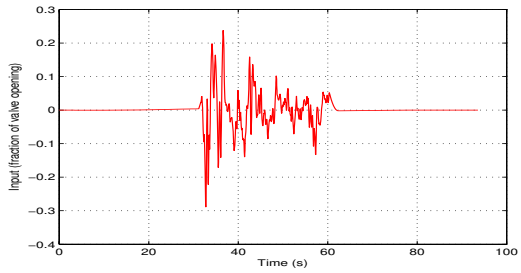

(e) Input

Fig. 3. Compatible trajectory of the shaketable for the 1940 El Centro accelerogram

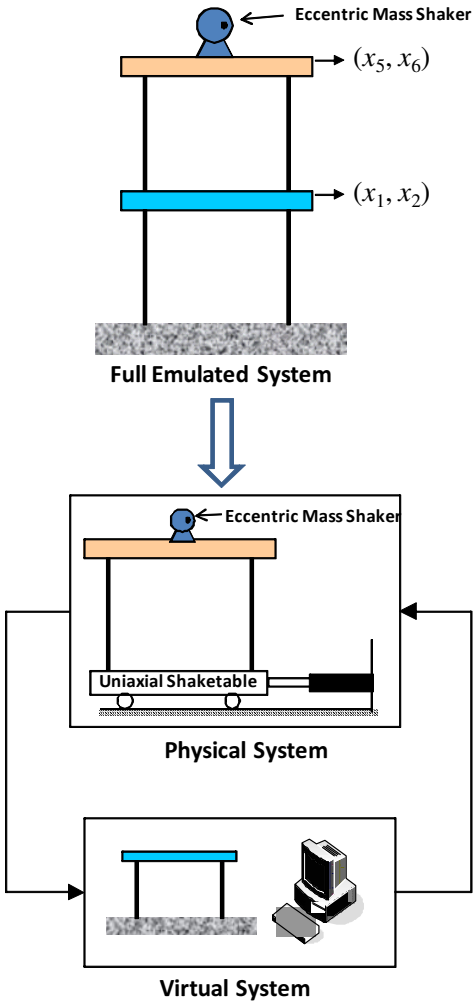

Fig. 4. Hybrid system explored

C. Desired Periodic Trajectory

The trajectory we desire of the hybrid system is the periodic trajectory of the emulated system obtained at steady state, when it is driven by $w(t) = w_d(t) = w_0 \sin(\Omega t)$. Let M, C and K be the mass, damping and stiffness matrices of the emulated structure. Define

$$\begin{bmatrix} X_{0,1} \\ X_{0,2} \end{bmatrix} = \left[(K - \omega^2 M) + j\Omega C\right]^{-1} \begin{bmatrix} 0 \\ w_0 \end{bmatrix}$$

and $x_{1,0} = |X_{0,1}|$, $\phi_1 = \arg(X_{0,1})$, $x_{5,0} = |X_{0,2}|$ and $\phi_2 = \arg(X_{0,2})$. Then the desired trajectory of the imitated system, $(x_{1,d}(\cdot), x_{2,d}(\cdot), x_{5,d}(\cdot), x_{6,d}(\cdot), w_d(\cdot))$ is given by $x_{1,d}(t) = x_{1,0}\sin(\Omega t + \phi_1)$, $x_{2,d}(t) = \Omega x_{1,0}\cos(\Omega t + \phi_1)$, $x_{5,d}(t) = x_{5,0}\sin(\Omega t + \phi_2)$, $x_{6,d}(t) = \Omega x_{5,0}\cos(\Omega t + \phi_2)$ and $w_d(t) = w_0 \sin(\Omega t)$.

D. Trajectory Optimization

As discussed above, letting $x(\cdot) = (x_3(\cdot), x_4(\cdot))$, we can pose the problem of finding compatible trajectories of the hybrid system in the form of a least squares optimization

problem as

$$\min_{(x(\cdot),u(\cdot))} \frac{1}{2}\int_0^T ||x(\tau)-x_d(\tau)||_Q^2 + ||u(\tau)-u_d(\tau)||_R^2\, d\tau + \frac{1}{2}||x(T)-x_d(T)||_{P_1}^2$$

Subject to

$$\begin{aligned}\dot{x}_3 &= f_3(x_{1,d}, x_{2,d}, x_3, x_4, u)\\ \dot{x}_4 &= f_4(x_{1,d}, x_{2,d}, x_3, x_4, u)\end{aligned} \tag{17}$$

with the periodic condition $x(T) = x(0)$, where $T = 2\pi/\Omega$. The strategy to solve this optimization problem is in two steps.

1) Solve the problem (17) with fixed initial conditions $x(0) = x_0$.
2) Consider the map $\pi : x_0 \mapsto x_T$ where $x_T = x(T)$ is obtained by solving the optimization problem with initial conditions x_0, and compute the fixed point of this map, i.e., solve for the initial conditions.

The optimization problem is solved using a projection operator-based descent algorithm [6]. An example calculation is shown in figure 5.

VII. SUMMARY AND CONCLUDING REMARKS

In the dynamic testing of structures, either with prescribed input such as an earthquake ground motion, or with computation-in-the-loop (i.e., hybrid simulation), the test system consisting of the physical test-piece, the actuators and sensors, controls, and other computations, constitutes a dynamic system that is different from the structure whose behavior is the focus of the test. We therefore ask if there are trajectories of the test system that are compatible with the desired trajectories of the structure tested. We formulate this problem as a nonlinear least-squares problem, and propose optimization strategies. We discuss the trajectory computation with two examples, seismic testing with prescribed ground motion, and hybrid simulation with a shaketable as the transfer system. The existence of compatible trajectories of the test system is a precondition for the design of online controls for dynamic tests. As an interesting additional contribution, we present an optimization-based strategy to compute consistent position and velocity curves for a desired accelerogram.

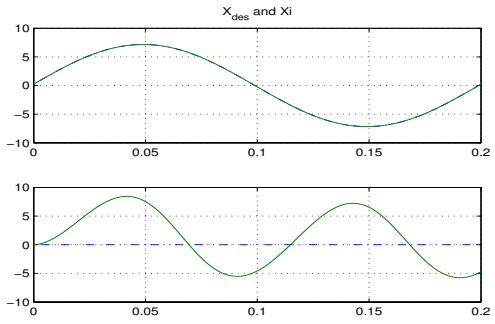

(a) Optimum trajectories of ΔP and ΣP for initial conditions $\Delta P = 0.2$ and $\Sigma P = 0$

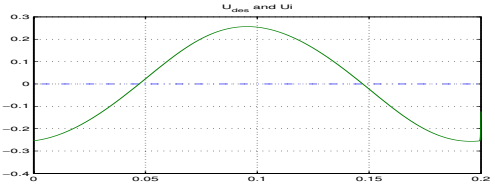

(b) Optimum input for initial conditions $\Delta P = 0.2$ and $\Sigma P = 0$

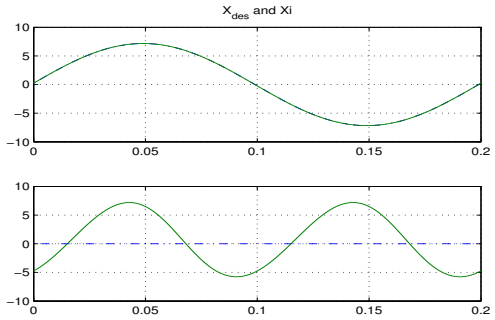

(c) Optimum trajectories of ΔP and ΣP for initial conditions $\Delta P = 0.3677$ and $\Sigma P = -4.7484$

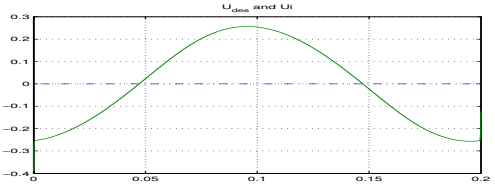

(d) Optimum input for initial conditions $\Delta P = 0.3677$ and $\Sigma P = -4.7484$

Fig. 5. Compatible trajectories of the hybrid system

VIII. ACKNOWLEDGMENTS

The authors gratefully acknowledge financial support from MTS Systems Corp.

REFERENCES

[1] M. S. Williams and A. Blakeborough, "Laboratory testing of structures under dynamic loads: an introductory review," *Philosophical Transactions of the Royal Society a-Mathematical Physical and Engineering Sciences*, vol. 359, no. 1786, pp. 1651–1669, 2001.

[2] H. E. Merritt, *Hydraulic control systems*. New York,: Wiley, 1967, [by] Herbert E. Merritt. illus. 24 cm.

[3] M. Jelali and A. Kroll, *Hydraulic servo-systems : modelling, identification, and control*, ser. Advances in industrial control. London ; New York: Springer, 2003.

[4] W. Borutzky, B. Barnard, and J. Thoma, "An orifice flow model for laminar and turbulent conditions," *Simulation Modelling Practice And Theory*, vol. 10, no. 3-4, pp. 141–152, 2002.

[5] S. Waydo, J. Hauser, R. Bailey, E. Klavins, and R. M. Murray, "Uav as a reliable wingman: A flight demonstration," *IEEE transactions on control systems technology*, vol. 15, no. 4, pp. 680–688, 2007.

[6] J. Hauser, "A projection operator approach to the optimization of trajectory functionals," in *15th IFAC World Congress*, Barcelona, 2002.